IMPROVED IDENTIFICATION OF THE PALMAR FIBROCARTILAGE OF THE NAVICULAR BONE WITH SALINE MAGNETIC RESONANCE BURSOGRAPHY

MICHAEL SCHRAMME, ZOLTAN KEREKES, STUART HUNTER, KRISZTINA NAGY, ANTHONY PEASE

Fibrocartilage degeneration is the earliest pathologic finding in navicular disease but remains difficult to detect, even with magnetic resonance (MR) imaging. We hypothesized that injection of the navicular bursa with saline would improve accuracy of MR imaging evaluation of palmar fibrocartilage. Thoracic limbs were collected from 11 horses within 6 h of death. Imaging was performed with a 1.5 T magnet using sagittal 2D proton density and transverse 3D FLASH sequences with fat saturation. For the purpose of determining sensitivity and specificity of the MR images, fibrocartilage was classified as normal or abnormal, based on combination of the findings of gross and microscopic pathology. Thickness of fibrocartilage was measured on histologic sections and corresponding transverse FLASH MR images before and after injection of saline. A paired Student's *t*-test was used for comparison of measurements. Partial thickness fibrocartilage loss was present in 6 of 22 limbs. Sensitivity of precontrast MR images for detection of lesions was 100% while specificity was 6%. Saline MR arthrography resulted in both sensitivity and specificity of 100% based on consensus review. Mean histologic fibrocartilage thickness was 0.75 ± 0.12 mm. Mean fibrocartilage thickness on precontrast transverse FLASH images was 0.93 ± 0.065 and 0.73 ± 0.09 mm on postsaline images. The histologic cartilage thickness was signficantly different from that in precontrast images ($P < 0.001$) but not in images acquired after saline injection ($P = 0.716$). Based on our results, and using pulse sequences as described herein, navicular fibrocartilage can only be evaluated reliably for the presence of partial thickness lesions after intrabursal injection of saline. *Veterinary Radiology & Ultrasound, Vol. 50, No. 6, 2009, pp 606–614.*

Key words: fibrocartilage, horse, MRI, navicular disease, saline contrast.

Introduction

DEGENERATION OF THE palmar fibrocartilage of the navicular bone is the earliest and most common pathologic finding in horses with navicular disease.[1–3] Early detection of fibrocartilage loss before bone degeneration occurs could result in earlier and more successful therapeutic intervention. Magnetic resonance (MR) imaging and ultrasonography, are the only imaging modalities that allow identification of cartilage, but it is difficult to detect degeneration of the navicular fibrocartilage even with MR imaging.[3,4] Therefore, diagnosis of early navicular disease will remain problematic unless contrast between fibrocartilage and adjacent tissue can be improved. Although gadolinium-containing compounds are the most commonly used MR contrast media, saline is also suitable in some instances and may lead to better contrast with the T1 signal generated by cartilage.[5] In addition, distension of the navicular bursa with fluid would physically push the palmar fibrocartilage of the navicular bone and the dorsal surface of the deep digital flexor tendon (DDFT) apart, which might improve the identification of intrabursal adhesions[6] and the definition of the respective surfaces of these structures. Better contrast and improved definition of the fibrocartilage layer should ultimately allow for easier detection of cartilage loss and improved measuring accuracy of cartilage thickness.

Our hypothesis was that injection of the navicular bursa with saline before MR imaging of the digit would result in improved accuracy in measuring the thickness of the palmar fibrocartilage of the navicular bone and improved sensitivity and specificity in detecting areas of fibrocartilage degeneration in comparison with MR imaging without saline.

Materials and Methods

Thoracic limbs from 11 horses were collected within 6 h of being euthanized for reasons other than the purpose of this study. Lateromedial, palmaro 45°proximal–palmarodistal oblique, and dorso 60°proximal–palmarodistal

From the College of Veterinary Medicine, North Carolina State University, Hillsborough Street 4700, Raleigh, NC 27606 (Schramme, Kerekes, Hunter), Faculty of Veterinary Science, Szent Istvan University, Istvan u. 2, Budapest, 1078 Hungary (Nagy), and the Department of Large Animal Clinical Sciences, Michigan State University, East Lansing, MI 48824 (Pease).

Address correspondence and reprint requests to Michael Schramme, at the above address. E-mail: michael_schramme@ncsu.edu

Received February 17, 2009; accepted for publication June 23, 2009.
doi: 10.1111/j.1740-8261.2009.01590.x

TABLE 1. Parameters Used in Pulse Sequences for Imaging Cadaver Limbs Using the Siemens Symphony High-Field MR Imaging System (1.5 T)

Pulse Sequence	TE (ms)	TR (ms)	FE	PE	NEX	FOV (cm)	Slice Thickness (mm)	Interslice Spacing	Flip Angle
Pilot (fl2d1)	5	15	256	128	1	50 × 50	5.0	7.5	40
2D PD TSE	14	3800	320	245	2	14 × 14	3.0	0.4	180
3D FLASH FS	10	36	256	256	1	12 × 12	2.0	−2.0	40

TE, echo time; TR, repetition time; FE, frequency encoding; PE, phase encoding; NEX, number of excitation; FOV, field of view; 2D PD TSE, 2-dimensional proton density turbo spin echo sequence; 3D FLASH FS, 3-dimensional fat saturated fast low angle shot sequence; fl2d1, 2-dimensional fast low angle shot sequence.

oblique digital radiographs of the front feet were obtained.* Using a published radiographic classification,[7] a numeric score was given to each navicular bone. Subsequently, the limbs were stored in a −40°C freezer until imaged. The limbs were then thawed in a water bath for 24 h before imaging. Imaging was performed with a 1.5 T high field MR unit† and consisted of a sagittal 2D proton density sequence (PD) with a slice thickness of 3 mm, and a fat saturated transverse 3D T1-weighted spoiled gradient echo sequence (FLASH) with a slice thickness of 2.0 mm (Table 1), both before and after injection of the navicular bursa with 6–10 ml 0.9% saline.‡ Injection of the navicular bursa was performed with an 88.9 mm long and 0.813-mm-diameter spinal needle,§ using the previously described virtual navicular position as a guide.[8] Initially the bursa was injected until resistance to injection was encountered or 6 ml of 0.9% saline was used, whichever came first. Subsequently, the amount of distension was evaluated by MR imaging. If the initial volume did not result in clear separation of the DDFT and the navicular bone, further 2 ml volume increments were injected until separation was achieved. MR images were interpreted using standard guidelines and the palmar fibrocartilage of the navicular bone was classified as normal or abnormal.[9]

Navicular bones were then removed and examined grossly. Fibrocartilage was stained with Indian ink to map areas of degeneration.[10,11] Digital photographs of the stained navicular bones were made. Subsequently the appearance of the palmar fibrocartilage was graded as no abnormalities, superficial fibrillation, partial thickness erosion, or full thickness erosion. Sagittal sections were made of each half and of the sagittal ridge area of each navicular bone, decalcified and stained with hematoxylin and eosin. Sections were examined microscopically and the appearance of the palmar fibrocartilage layer was graded as normal, abnormal without cartilage loss, abnormal with $<50\%$ of total fibrocartilage thickness loss, and abnormal with $>50\%$ of total fibrocartilage thickness loss.

For the purpose of measuring the thickness of the fibrocartilage layer, sagittal histologic sections of the central part of the medial half, the central part of the lateral half, and the sagittal ridge region of the navicular bones were used.

Calibrated digital images of each slide were obtained by use of a microscope linked to an optical digital camera¶ with electronic calipers at × 10 magnification. Thickness measurements were performed on the calibrated digital photographs perpendicular to the fibrocartilage surface at the standard sites by use of image analysis software.‖ Thickness measurements were also performed before and after injection of saline, on corresponding transverse FLASH MR images using a specialized program.‖ Boundaries between articular cartilage, subchondral bone, and intrabursal fluid were located on MR images as sharp alterations in pixel intensity. Pixel intensity limits were used on the basis of data from another study[12] and the authors' experience with other joints. Each measurement was performed 3 times and the mean was used for comparison. Magnetic resonance and histologic thickness measurements were compared using a paired Student's *t*-test.**

For determining sensitivity and specificity of MR imaging, the fibrocartilage layer of each navicular bone was classified as normal or abnormal, based on combination of the findings of gross and microscopic pathology. Only fibrocartilage with gross or microscopic evidence of tissue loss, either partial or full thickness, was considered abnormal for the purpose of this study. Microscopic cartilage abnormalities such as mild fibrillation of the surface layer, chondrocyte hypertrophy, chondrocyte proliferation, chondrone formation, or proteoglycan depletion were not classified as abnormal for the purpose of this imaging study. The MR images were evaluated independently by a board-certified radiologist and a board-certified surgeon with experience in MR image interpretation; reviewers were not made aware of the image sequence or whether the

*Eklin Mark DR System, Eklin Medical Systems Inc., Santa Clara, CA 95054.

†Siemens, Malvern, PA.

‡0.9% Sodium chloride injection, USP, 500 ml; Hospira Inc., Lake Forest, IL 60045.

§BD Spinal needle 20GA 3.5 in; BD Medical, Franklin Lakes, NJ.

¶QIMAGING Micropublisher 5.0 RTV, Surrey, BC, Canada.

‖Scion Image Alpha 4.0.3.2, Scion Corp., Frederick, MD.

**R 2.7.2. Statistical software; R Development Core Team 2007, Boston, MA.

navicular bursa had been injected. Subsequently, evaluations from each reviewer were compared and a consensus was reached regarding allocation of an MR imaging grade to each navicular bone. These were then compared with gross and histologic findings to determine what signal characteristics were indicative of fibrocartilage degeneration. The presence of hyperintense signal adjacent to a palmar depression in the middle third of the sagittal ridge was regarded as fluid pooling in a normal anatomic midsagittal ridge synovial fossa. This was not considered as an abnormal finding unless other MR imaging evidence of degenerative change was identified in the same area. Sensitivity, specificity, accuracy, as well as positive and negative predictive values were then calculated for each image sequence using standard calculations.

Results

The mean radiographic score was 1.32. Eight bones were excellent (grade 0), 1 was good (grade 1), and 11 were fair (grade 2). Only 2 navicular bones were graded as poor (grade 3; horse 11). None of the navicular bones were graded as bad (grade 4).

In all limbs, we found that the uniform hyperintense layer between the hypointense palmar cortex of the navicular bone and the dorsal surface of the hypointense DDFT, could be separated on transverse FLASH images into 2 distinct thin hyperintense layers by intrabursal injection of saline. Injected saline was seen interposed as a thin hypointense layer between both hyperintense tissue layers (Fig. 1).

Rupture of the synovial membrane occurred in 11 cadaver limbs and was detected by the presence of saline signal intensity in the distal interphalangeal joint space, the digital synovial sheath or, in 2 limbs, in a subcutaneous location at the palmarodistal aspect of the middle phalangeal region. When it was not possible to distend the bursa satisfactorily because of synovial membrane rupture and subcutaneous fluid leakage, limbs were not included for postsaline MR image analysis (2 limbs).

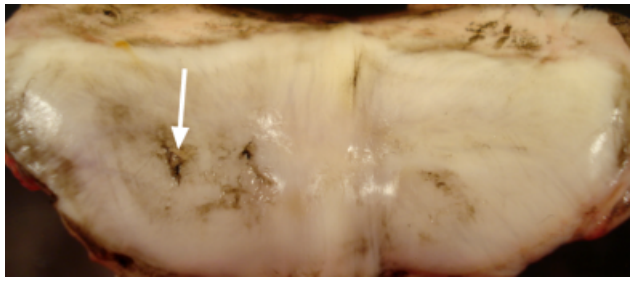

FIG. 2. Gross appearance of the flexor surface of the left navicular bone of a horse following application of Indian ink stain. Areas of partial thickness fibrocartilage loss (stained brown) are visible on the lateral surface (white arrow). Lateral is to the left of the image. Compare with Fig. 7.

The mean histologic fibrocartilage thickness was 0.75 ± 0.12 mm. On survey transverse FLASH MR images, mean fibrocartilage thickness was measured as 0.93 ± 0.065 mm. On postcontrast transverse FLASH MR images, mean fibrocartilage thickness was 0.73 ± 0.09 mm. The difference between histologic and noncontrast MR image assessment of fibrocartilage thickness was statistically significant ($t_{64} = -9.943$, $P < 0.001$, 95% confidence interval -0.215 to 0.143). Thus, in precontrast MR images the thickness of fibrocartilage was overestimated compared with histology. However, there was no signficant difference between postsaline MR image measurements and the actual fibrocartilage thickness measured histologically ($t_{53} = 0.366$, $P = 0.716$, 95% confidence interval -0.034 to 0.049).

During gross and microscopic pathologic examination, fibrocartilage lesions were identified in 6 of 22 limbs. All areas of fibrocartilage loss in those 6 navicular bones were graded as partial thickness and occurred either on the lateral or medial palmar surface, on the sagittal ridge or in several areas simultaneously (Fig. 2). In 2 limbs, a focal adhesion was present between the dorsal surface of the DDFT and an area of partial thickness fibrocartilage loss

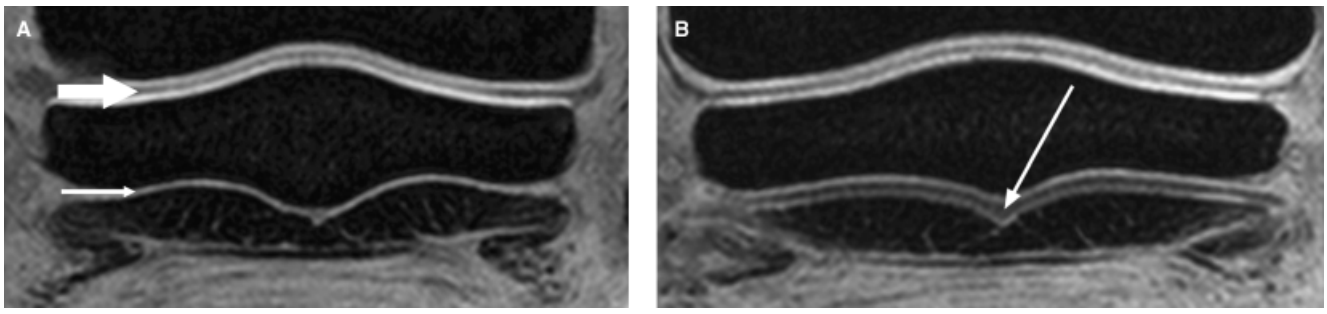

FIG. 1. (A) Three-dimensional transverse T1-weighted FLASH images with fat saturation of the navicular bone area before saline injection into the navicular bursa. One hyperintense layer separates the dorsal surface of the deep digital flexor tendon (DDFT) from the palmar surface of the navicular bone (small arrow). A thin hypointense layer of synovial fluid can be seen in the palmar pouch of the distal interphalangeal joint (large arrrow). (B) Three-dimensional transverse T1-weighted FLASH images with fat saturation of the navicular bone area after saline injection into the navicular bursa. Two distinct thin hyperintense layers are separated by a thin hypointense layer of intrabursal saline (white arrow). The T1 signal similarity of these hyperintense layers suggests that fibrocartilage may also be present on the dorsal aspect of the DDFT.

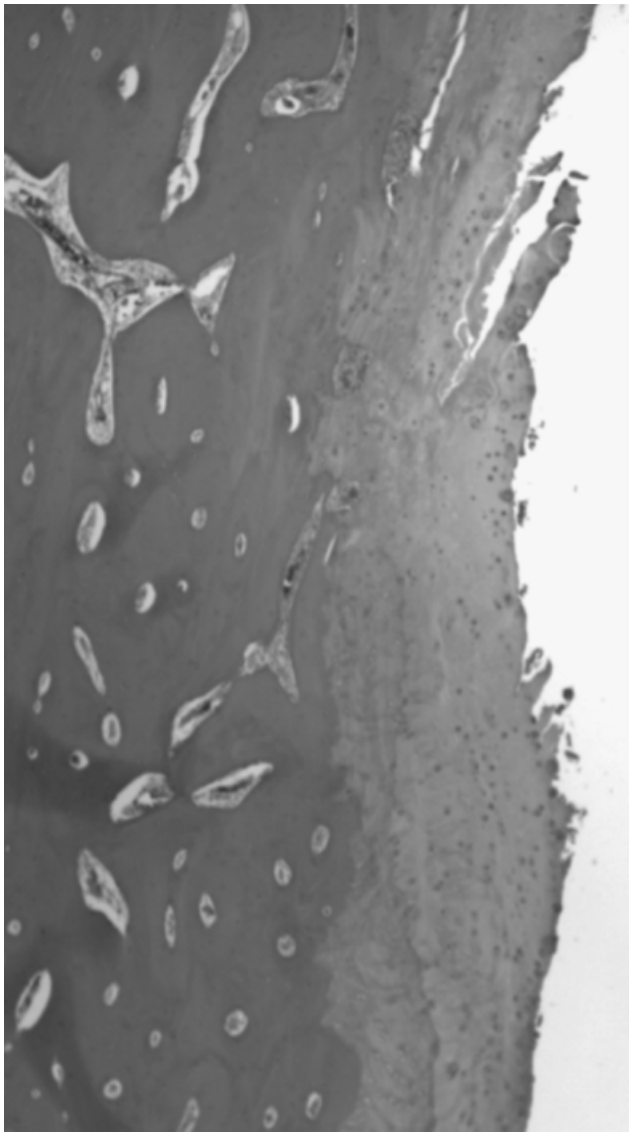

FIG. 3. Sagittal section with hematoxilin and eosin stain (× 4 magnification) of the sagittal ridge area of the left navicular bone of horse 11. There is a central area with surface fibrillation, crevicing and partial thickness loss of fibrocartilage. Dorsal is to the left and palmar is to the right.

on the palmar surface of the navicular bone. In 5 of 6 navicular bones, fibrocartilage loss involved $<50\%$ of the fibrocartilage layer thickness (Fig. 3), while in 1 of 6 navicular bones, a fibrocartilage erosion of $>50\%$ depth was present.

Survey MR image abnormalities of the palmar fibrocartilage were perceived in 21 of 22 navicular bones on sagittal PD sequences. These abnormalities consisted mainly of the presence of a focal signal hyperintensity at the level of the fibrocartilage layer adjacent to the palmar cortical surface of the lateral or medial half of the navicular bone in 18 bones (Fig. 4), loss of palmar cortical outline and focal or generalized signal increase within the flexor cortex lateral

FIG. 4. Parasagittal 2D PD image of the left navicular bone of horse 10, obtained 2 cm medial to the center of the palmar sagittal ridge. There is a focal signal hyperintensity at the level of the fibrocartilage layer adjacent to the palmar cortical surface (white arrow) that was thought to reflect the presence of fluid pooling at the site of a localized palmar fibrocartilage erosion. Pathologically, there were no fibrocartilage abnormalities medial to the sagittal ridge (see Fig. 2). Given these results, such a focal hyperintensity cannot be considered as a reliable predictor of fibrocartilage disease.

or medial to the sagittal ridge region in 10 bones (Fig. 5), and the presence of a focal signal hyperintensity in a palmar depression in the middle third of the sagittal ridge of the navicular bone accompanied by local loss of cortical

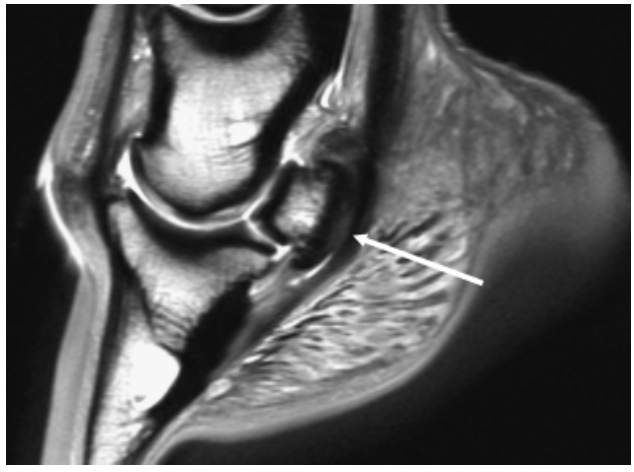

FIG. 5. Sagittal 2D PD image of the left navicular bone of horse 11 adjacent to the sagittal ridge without saline injection into the navicular bursa. There is loss of trabecular structure, focal signal increase in the medullary cavity, thickening and endosteal irregularity of the flexor cortex of the navicular bone. In addition, there is loss of palmar cortical outline and generalized signal increase within the flexor cortex immediately lateral to the sagittal ridge region. Pathologically, there was localized loss of fibrocartilage and cortical bone from the palmar surface of the navicular bone in this location.

FIG. 6. Sagittal 2D PD image of the left navicular bone of horse 6 at the sagittal ridge without saline injection into the navicular bursa. A focal signal hyperintensity is present in a palmar depression in the middle third of the sagittal ridge of the navicular bone accompanied by an irregular outline to the endosteal surface of the flexor cortex with adjacent thickening of medullary trabeculae (white arrow). These changes were regarded as indicative of fluid pooling in a palmar depression in the navicular bone with adjacent cortical and medullary remodelling. No pathologic abnormalities were found. There was no evidence of a palmar synovial fossa in the sagittal ridge. Given these results, such a focal hyperintensity cannot be considered as a reliable predictor of fibrocartilage disease.

bone, irregular outline to the endosteal surface and adjacent thickening of medullary trabeculae in 5 bones (Fig. 6). A focal adhesion between the dorsal surface of the DDFT and a palmar depression in the middle third of the sagittal ridge of the navicular bone was present in 1 horse. At least 2 of these perceived MR abnormalities occurred simultaneously in 11 navicular bones. None of these navicular bones appeared abnormal on survey transverse FLASH images.

After injection of saline into the navicular bursa, MR image abnormalities of the palmar fibrocartilage were perceived in 2 of 22 navicular bones on sagittal PD sequences and 6 of 22 navicular bones on transverse FLASH sequences. Two of these navicular bones had palmar fibrocartilage abnormalities that were seen on both sagittal PD and transverse FLASH postsaline sequences. The most common postsaline fibrocartilage MR image abnormality was the presence of one or more focal discontinuities in the homogenous signal of the fibrocartilage layer, where the normal, relatively hyperintense cartilage signal was replaced by hypointense saline signal on the transverse FLASH sequence (Fig. 7). This occurred in 6 of 6 bones with postsaline MR abnormalities and was considered indicative for the presence of focal loss of cartilage with accumulation of saline in the tissue defect. In addition, the presence of a focal soft tissue adhesion between the dorsal surface of the DDFT and an area of cartilage degeneration at the palmar surface of the navicular bone could be clearly seen as a linear signal hypointensity traversing the hyperintense, saline-distended bursal space on sagittal PD sequences in 2 limbs (Fig. 8). In 1 of these limbs, the adhesion resulted in a focal filling defect in the navicular bursa on the transverse FLASH sequence, resulting in a signal discontinuity of the hypointense saline layer (Fig. 9).

Using the abnormalities described above, the sensitivity, specificity, and accuracy were determined for the sagittal PD and the transverse FLASH sequences separately, both before and after use of saline. For the sagittal PD sequence, the sensitivity, specificity, and accuracy were 100%, 6%, and 32%, respectively, before saline, and 33%, 100%, and 82% after saline administration. For the transverse FLASH sequence, the sensitivity, specificity and accuracy

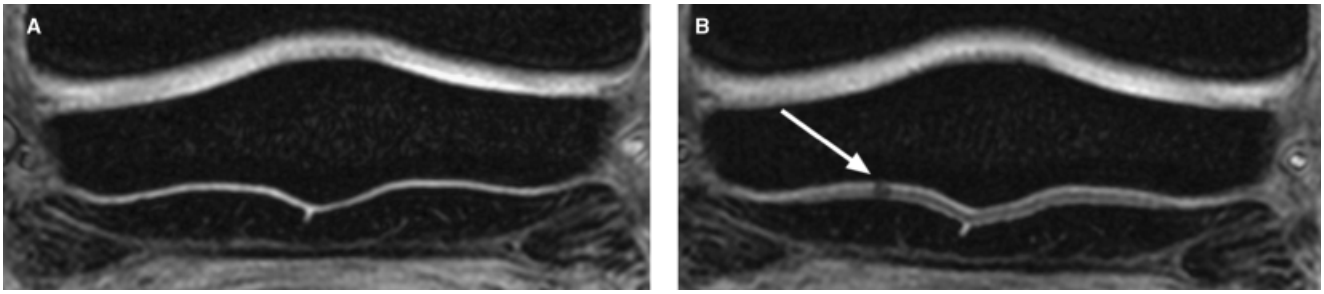

FIG. 7. (A) 3D transverse T1-weighted FLASH image with fat saturation of the middle third of the left navicular bone of horse 10. There is a thin, homogeneous layer of high signal intensity and uniform thickness along the palmar surface of the navicular bone representative of fibrocartilage (white arrow). Compare with Fig. 2. Lateral is to the left. (B) 3D transverse T1-weighted FLASH image with fat saturation of the middle third of the left navicular bone of horse 10 after saline injection into the navicular bursa. Image location corresponds to that of (A). A focal discontinuty is present in the high intensity fibrocartilage layer, where the normal, high intensity cartilage signal is replaced by hypointense saline signal in an area of focal cartilage loss on the lateral surface of the bone (white arrow). Compare with Fig. 2. Lateral is to the left.

FIG. 8. Sagittal 2D PD image of the sagittal ridge area of the left navicular bone of horse 4 after saline injection into the navicular bursa. A focal soft tissue adhesion is visible between the dorsal surface of the deep digital flexor tendon and an area of cartilage degeneration, as a linear signal hypointensity traversing the hyperintense, saline-distended bursal space (white arrow).

were 0%, 100%, and 73%, respectively, before saline, and 100%, 100%, and 100% after saline administration.

When both the sagittal PD and the transverse FLASH sequences were combined, sensitivity of survey MR imaging for detection of fibrocartilage lesions was 100% but specificity was only 6%. The false-positive rate of survey MRI was 94%, while the false-negative rate was 0%. The positive predictive value (PPV) was 28% and the negative predictive value (NPV) was 100%. After administration of saline into the navicular bursa, both sensitivity and specificity were graded as 100%, and both false-positive and false-negative rates were 0. The PPV was 100% and the NPV was 100%.

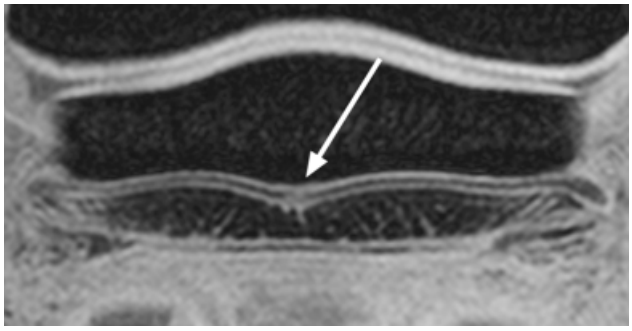

FIG. 9. 3D transverse T1-weighted FLASH image with fat saturation of the left navicular bone of horse 7 after saline injection into the navicular bursa. There is a focal bursal filling defect at the level of the sagittal ridge, resulting in a signal discontinuity of the hypointense saline layer, representing an adhesion (white arrow).

Discussion

Degeneration of the palmar fibrocartilage layer of the navicular bone and the dorsal surface of the DDFT is believed by many to be the initiating factor of classic navicular disease.[2,13,14] This should not be confused with the presence of a palmar depression in the middle third of the sagittal ridge, that has previously been described as a mid-ridge synovial fossa and is considered a normal anatomic variant.[2] Radiography is incapable of allowing fibrocartilage or tendon tissue to be assessed accurately due to the lack of contrast resolution and superimposition of structures. Identification of fibrocartilage degeneration before radiographic abnormalities develop in the navicular bone is therefore key to early diagnosis of navicular disease. Early diagnosis should improve the opportunity for preventive and disease-reversing therapies. Although it was hoped that MR imaging would provide this opportunity, the reliability of cartilage imaging with clinical MR imaging has so far produced mixed results, not only in the distal limbs of horses[15] but also in the human knee. Comparisons between MR imaging and arthroscopic evaluation of the human knee have indicated a better correlation between the prediction and finding of meniscal lesions than of articular cartilage defects.[16–18]

Nevertheless, it has been stated that spoiled gradient echo sequences (SPGR), with or without fat saturation, are most suitable for evaluation of articular cartilage in horses.[12] This agrees with our results with the 3D FLASH sequence, which is Siemens' equivalent of General Electric's SPGR sequence. In addition, we have also found the 2D PD sequences clinically useful for articular cartilage evaluation in the digit. Therefore we elected to evaluate both the sagittal 2D PD sequence and the transverse 3D FLASH sequence with fat saturation for the purpose of this study. Even though it has been stated that the use of these sequences allows for accurate assessment of articular cartilage,[12,19] others have reported that evaluation of the palmar fibrocartilage of the navicular bone remains difficult.[4] The palmar fibrocartilage of the navicular bone has intermediate signal intensity, is the thinnest cartilage layer in the limb, and there is no adjacent layer of synovial fluid to provide contrast due to the tight apposition between the articular cartilage and the DDFT. In our experience, this tight apposition is maintained in most horses, even when considerable effusion of the navicular bursa is present. Effusion tends to result first in distension of the proximolateral and proximomedial pouches of the navicular bursa rather than separation of the opposing surfaces of the DDFT and the navicular bone.

In view of these difficulties, intrabursal contrast medium was used to improve visualization of the fibrocartilage layer. It was recently reported that injection of 6 ml of fluid in the navicular bursa is sufficient for separation of the palmar surface of the navicular bone from the dorsal surface of the DDFT.[6] In our experience, the volume required to obtain this degree of distension was variable but frequently closer to 10 ml than 6 ml. Adding a fluid volume of 10 ml to the navicular bursa carries a significant risk of rupturing the synovial membrane. Contrary to our expectation, it was not easy to detect when the point of rupture was imminent simply from the amount of back pressure on the syringe. It is unknown what the clinical consequences of synovial membrane rupture are likely to be for the navicular bursa, but we have observed iatrogenic rupture of the navicular bursa during positive contrast bursography of 2 other horses with puncture wounds to the foot and no untoward long-term effects were observed. It is unclear why we were frequently unable to obtain satisfactory distension of the navicular bursa with the volumes reported in another study.[6] Frozen storage of our specimens may have resulted in decreased pliability of the soft tissues, thereby requiring higher fluid pressure to open the potential space between the DDFT and the palmar surface of the navicular bone. We therefore do not recommend the use of >6 ml of saline to distend the navicular bursa in live horses.

The standard for MR contrast arthrography are gadolinium compounds and these agents generate T1 signal hyperintensity and offer little contrast with the intermediate intensity signal of fibrocartilage on T1-weighted sequences like FLASH/SPGR. The use of MR arthrography with gadolinium compounds has led to limited success in improving the detection of cartilage lesions in man.[5] Better cartilage contrast was obtained following injection of saline into the synovial space,[5,20] as the hypointense signal generated by saline is markedly different from the intermediate high intensity signal of fibrocartilage on T1-weighted sequences. As can be seen in Fig. 1, our observations were in agreement with these findings.

Following introduction of hypointense contrast medium in the bursa, there were 2, adjacent, distinct, T1 hyperintense tissue layers in the navicular bursa, one on the palmar surface of the navicular bone and another on the dorsal surface of the DDFT (Fig. 1). The T1 signal similarity of these layers suggests that both contain fibrocartilage. Tendons have been shown to contain fibrocartilage in areas of compression associated with a change in the direction of the pull around bony prominences, as occurs over the palmar aspect of the proximal and distal sesamoid bones.[21] While the dorsal 20–30% of the DDFT immediately proximal to the navicular bursa consists of a pale-staining, well-delineated zone of fibrocartilage rich in elastic fibers, the tendon lacks a dorsal fibrocartilage zone at more distal levels.[22] The reason for the presence of a thin layer of T1 hyperintense signal on the dorsal surface of the DDFT at the level of the navicular bone is therefore unclear, unless a distal offshoot exists from the more substantial dorsal fibrocartilage layer proximal to the navicular bursa.

The palmar fibrocartilage layer of the navicular bone could only be evaluated separately from the T1 hyperintense tissue layer on the dorsal surface of the DDFT after the bursa had been injected with a T1 hypointense contrast agent like saline. Without this visual separation of both layers, it was impossible to determine whether MR signal abnormalities interposed between the palmar surface of the navicular bone and the dorsal surface of the DDFT emanated from either one or the other. In addition, thickness measurements on survey transverse FLASH MR images of the hyperintense tissue layer between the dorsal surface of the DDFT and the palmar surface of the navicular flexor cortex resulted in overestimation of the actual fibrocartilage thickness because the measurement encompassed 2 tissue layers rather than 1. After injection of saline in the navicular bursa, the MR measurements of the fibrocartilage layer closely approximated the true cartilage thickness as measured histologically. Others have also found excellent agreement between histomorphometric (1.446 ± 0.311 mm) and MR imaging (1.436 ± 0.303 mm) measurements of articular cartilage thickness of the intermediate and third carpal bones of horses, but only when the calcified cartilage layer was included in the histomorphometric measurement.[12] Without the calcified cartilage, articular cartilage thickness of carpal bones was 0.921 ± 0.267 mm.[12] A calcified cartilage layer was not observed on the palmar surface of the navicular bones in this study. The palmar fibrocartilage of the navicular bone was thinner than the articular cartilage of the intermediate carpal bone. This difference places the thickness of navicular fibrocartilage close to the spatial resolution of the MR images acquired in this study, where 1 mm equalled 4.7 pixels and 1 pixel corresponded to a mean distance of 0.21 mm. Occasionally this made recognition of the boundary between fibrocartilage and subchondral bone or bursal fluid difficult, as the transition would have occurred in the same pixel and accuracy might have been lost due to volume averaging. A higher spatial resolution with smaller pixel size would have improved accuracy, especially for a tissue layer as thin as navicular fibrocartilage; however, this would not be practical because it would dramatically increase scan time and no longer be clinically relevant.

Other problems can arise when trying to measure cartilage accurately. There are inherent difficulties associated with MR imaging of tissue interfaces when long echo times are used. The preferential loss of signal from the deep layers of cartilage with long echo times obscures the interface

between cartilage and subchondral bone, which makes it difficult to obtain an accurate measurement of cartilage thickness or volume. In one study there was only a 52% accuracy rate with conventional T2-weighted spin echo (SE) sequences to detect naturally occurring lesions in the patellofemoral joints of cadavers.[23] Moreover, due to magnetic susceptibility artifacts from the deep layer of cartilage and cancellous subchondral bone, some gradient echo (GRE) sequences obscure the cartilage bone interface, again making quantification of cartilage difficult.[24] Clinical studies using such sequences have reported poor results with sensitivities ranging from a low of 31% to a high of 87%.[25]

The poor accuracy of noncontrast MR images for detection of cartilage damage in this study confirms the previously described difficulties.[3] Standard interpretation guidelines propose that focal hyperintensities in T2- or PD-weighted images interposed between the dorsal surface of the DDFT and the palmar surface of the navicular bone represent accumulation of synovial fluid in focal depressions in the palmar surface caused by localized fibrocartilage loss or by a normal depression in the middle third of the sagittal ridge (palmar synovial fossa).[9] However, based on our work focal hyperintensities in the fibrocartilage layer could not be considered as reliable predictors of fibrocartilage disease (accuracy 32%) and interpretation of fibrocartilage disease according to the standard guidelines resulted in an unacceptably high false-positive rate (94%). It must be concluded that focal signal PD hyperintensities may occur due to pooling of bursal fluid at the level of the fibrocartilage layer of the navicular bone due to normal anatomic variation in the shape of the palmar border of the navicular bone without evidence of fibrocartilage loss. Loss of the palmar outline and irregular signal increase of the flexor cortex adjacent to the sagittal ridge area of the navicular bone was also a common finding on sagittal PD sequences of normal navicular bones. This signal change is most likely caused by partial volume averaging effect when the slice direction is no longer perpendicular to the palmar surface of the navicular bone, as typically occurs on sagittal slices close to the sagittal ridge region of the navicular bone.[26] A diagnosis of fibrocartilage degeneration based solely on the presence of a focal T2 or PD hyperintensity at the palmar surface of the navicular bone is therefore unreliable. This partial volume averaging effect is less likely to affect T2- or PD-weighted sequences in a transverse imaging plane because of the different proximodistal configuration of the palmar surface of the navicular bone. In addition, it is possible that different specifications to the PD sequence, such as longer echo times and addition of fat suppression would have improved conspicuity of cartilage lesions by improving delineation of the interface between cartilage and synovial fluid. Consequently, the sensitivity and specificity of survey PD sequences for cartilage lesions might have been better if different specifications had been used for these sequences. However, we set out to evaluate the sequences used in our clinical protocol, for which different specifications were used to maximize the diagnostic value for a variety of tissues.

Moreover, only 2 navicular bones in this study had radiographic evidence of disease. Therefore, in the majority of limbs only mild fibrocartilage lesions, comprising $<50\%$ depth, were available for study. It is likely that the accuracy of noncontrast-enhanced MR images would have been better for full thickness fibrocartilage lesions. In a study of cartilage defects in canine femoral condyles, a lesion width of 3 mm and depth of 0.4 mm was the smallest detectable cartilage lesion size when using a T1-weighted FLASH 3D sequence with anisotropic voxels of $0.3 \times 0.3 \times 0.8$ mm.[27] The average thickness of normal fibrocartilage in our study was 0.75 mm. As most areas of fibrocartilage loss comprised $<50\%$ of the fibrocartilage thickness, their depth was likely to be close to the threshold of the smallest detectable lesion size.[27] In fact, the smallest detectable lesion in our study could be expected to be larger than the one defined in canine stifles, as the FLASH sequence in our study had a larger voxel size ($0.5 \times 0.5 \times 2$ mm).

The addition of intrabursal saline as contrast medium markedly improved the ability to detect cartilage lesions. Contrast bursography eliminated false-positive findings on the sagittal PD images and all areas of focal cartilage loss could be seen on the transverse FLASH images. Of the sequences and imaging planes examined, the transverse FLASH after injection of the navicular bursa with saline was the most sensitive, specific, and accurate technique for detection of focal fibrocartilage loss from the palmar surface of the navicular bone. However, combination of both postsaline sagittal PD and postsaline transverse FLASH sequences made it possible to detect 2 adhesions between the navicular bone and the DDFT that were harder to detect on the transverse FLASH sequence alone, because of the superior contrast between saline and adhesion tissue on the sagittal PD sequence.

Although it is difficult to evaluate partial thickness lesions of the palmar fibrocartilage of the navicular bone without intrabursal saline, the technique is not without its difficulties. Following precontrast images, the horse needs to be removed from the magnet, the foot aseptically prepared for injection, a needle introduced through the DDFT, the needle position evaluated, and the navicular bursa injected without causing synovial rupture. Subsequently, the RF coil needs to be reapplied and new localizer images acquired. This increases time under anesthesia and may result in longer and more expensive MR examinations. Alternatively, for horses with suspected navicular pain, the navicular bursa could be injected outside the magnet room before imaging. The loss of

survey images would be compensated for by a more sensitive, specific, and accurate MR examination for the diagnosis of early-stage navicular disease but might preclude the detection of bursal distension caused by navicular bursitis.

In conclusion, partial thickness fibrocartilage lesions of the navicular bone can be identified with a high degree of accuracy following injection of a T1 hypointense contrast medium like saline into the navicular bursa.

ACKNOWLEDGMENT

The authors wish to thank Susan McCullough for performing the MRI studies.

REFERENCES

1. Colles CM. Navicular disease and its treatments. In Pract 1982;4: 29–36.

2. Wright I, Kidd L, Thorp B. Gross, histological and histomorphometric features of the navicular bone and related structures in the horse. Equine Vet J 1998;30:220–234.

3. Schramme MC, Murray RM, Blunden TS, Dyson SJ. A comparison between magnetic resonance imaging, pathology and radiology in 34 limbs with navicular syndrome and 25 control limbs. *Proceedings of the 51st Annual Convention of the American Association of Equine Practitioners*, Seattle, WA, December 3–7, 2005; 348–358.

4. Widmer WR, Buckwalter KA, Fessler JF. The use of radiography, computed tomography and magnetic resonance imaging for evaluation of navicular syndrome in the horse. Vet Radiol Ultrasound 2000;41:108–116.

5. Chandnani VP, Ho C, Chu P, Trudell D, Resnick D. Knee hyaline cartilage evaluated with MR imaging: a cadaveric study involving multiple imaging sequences and intraarticular injection of gadolinium and saline solution. Radiology 1991;178:557–561.

6. Maher MC, Werpy NM, Goodrich LR, McIlwraith CW. Distension of the Navicular Bursa to Determine the Presence of Adhesions Using Magnetic Resonance Imaging. *Proceedings of the 54th Annual Convention of the American Association of Equine Practitioners*, San Diego, CA, December 6–10, 2008; 460–461.

7. Dik KJ, van den Broek J. Role of navicular bone shape in the pathogenesis of navicular disease: a radiological study. Equine Vet J 1995;27:390–393.

8. Schramme MC, Boswell JC, Hamhoughias K, Toulson K, Viitanen M. An in vitro study to compare 5 different techniques for injection of the navicular bursa in the horse. Equine Vet J 2000;32:263–267.

9. Murray RM, Schramme MC, Dyson SJ, Branch MV, Blunden TS. Magnetic resonance imaging characteristics of the foot in horses with palmar foot pain and control horses. Vet Radiol Ultrasound 2006;47:1–16.

10. Cantley CE, Firth EC, Delahunt JW, Pfeiffer DU, Thompson KG. Naturally occurring osteoarthritis in the metacarpophalangeal joints of wild horses. Equine Vet J 1999;31:73–81.

11. Brommer H, van Weeren PR, Brama PA. New approach for quantitative assessment of articular cartilage degeneration in horses with osteoarthritis. Am J Vet Res 2003;64:83–87.

12. Murray RC, Branch MV, Tranquille C, Woods S. Validation of magnetic resonance imaging for measurement of equine articular cartilage and subchondral bone thickness. Am J Vet Res 2005;66:1999–2005.

13. Hickman J. Navicular disease, what are we talking about? Equine Vet J 1989;21:395–398.

14. Pool R, Meagher D, Stover S. Pathophysiology of navicular syndrome. Vet Clin N Am Equine Pract 1989;5:109–129.

15. Schramme MC, Murray RC, Dyson SJ, Boswell J. Magnetic resonance imaging of the foot. In: Floyd A, Mansmann R (eds): Equine podiatry. St. Louis, MO: W. B. Saunders, 2007;175–188.

16. Guckel C, Jundt G, Schnabel K, Gacther A. Spin-echo and 3D gradient-echo imaging of the knee joint: a clinical and histopathological comparison. Eur J Radiol 1995;21:25–33.

17. Munk B, Madsen F, Lundorf E, et al. Clinical magnetic resonance imaging and arthroscopic findings in knees: a comparative prospective study of meniscus anterior cruciate ligament and cartilage lesions. Arthroscopy 1998;14:171–175.

18. Kawahara Y, Uetani M, Nakahara N, et al. Fast spin-echo MR of the articular cartilage in the osteoarthrotic knee. Correlation of MR and arthroscopic findings. Acta Radiol 1998;39:120–125.

19. Link TM, Stahl R, Woertler K. Cartilage imaging: motivation, technique, current and future significance. Eur Radiol 2007;17:1135–1146.

20. Yao L, Gentili A, Seeger LL. Saline versus gadolinium-enhanced magnetic resonance arthrography of porcine cartilage. Acad Radiol 1997;4:127–131.

21. Smith R. Pathophysiology of tendon injury. In: Ross MW, Dyson SJ (eds): Diagnosis and management of lameness in the horse. St. Louis, MO: W. B. Saunders, 2003;619–632.

22. Blunden A, Dyson SJ, Murray RM, Schramme MC. Histopathology in horses with chronic palmar foot pain and age-matched controls. Part 2: the deep digital flexor tendon. Equine Vet J 2006;38:23–27.

23. Recht MP, Kramer J, Marcelis S, et al. Abnormalities of articular cartilage in the knee: analysis of available MR techniques. Radiology 1993;187:473–478.

24. Heron CW, Calvert PT. Threedimensional gradient-echo MR imaging of the knee: comparison with arthroscopy in 100 patients. Radiology 1992;183:839–844.

25. Wojtys E, Wilson M, Buckwalter K, Braunstein E, Martel W. Magnetic resonance imaging of knee hyaline cartilage and intraarticular pathology. Am J Sports Med 1987;15:455–463.

26. Cohen ZA, McCarthy DM, Kwak SD, et al. Knee cartilage topography, thickness, and contact areas from MRI: in-vitro calibration and in-vivo measurements. Osteoarth and Cart 1999;7:95–109.

27. Flatz K, Glaserù C, Reiser M, Matis U. Detection and evaluation of cartilage defects in the canine stifle joint—an ex-vivo study using high-resolution high-field MRI. *Proceedings of the 13th ESVOT Congress*, Munich, Germany, September 7–10, 2006; 227.